Eur Biophys J (2003) 32: 370–380
DOI 10.1007/s00249-003-0279-x

ARTICLE

Alexander Schuster · Jean-Louis Bény
Jean-Jacques Meister

Modelling the electrophysiological endothelial cell response to bradykinin

Received: 3 October 2002 / Revised: 12 December 2002 / Accepted: 13 December 2002 / Published online: 20 February 2003

Abstract The goal of the present study is to construct a biophysical model of the coronary artery endothelial cell response to bradykinin. This model takes into account intracellular Ca^{2+} dynamics, membrane potential, a non-selective cation channel, and two Ca^{2+}-dependent K^+ channels, as well as intra- and extracellular Ca^{2+} sources. The model reproduces the experimental data available, and predicts certain quantities which would be hard to obtain experimentally, like the individual K^+ channel currents when the membrane potential is allowed to freely evolve, the implication of epoxyeicosatrienoic acids (EETs), and the total K^+ released during stimulation. The main results are: (1) the large-conductance K^+ channel participates only very little in the overall response; (2) EETs are required in order to explain the experimental current-potential relationships, but are not an essential component of the bradykinin response; and (3) the total K^+ released during stimulation gives rise to a concentration in the intercellular space which is of millimolar order. This concentration change is compatible with the hypothesis that K^+ contributes to the endothelium-derived hyperpolarizing factor phenomenon.

A. Schuster (✉) · J.-J. Meister
Cellular Biophysics and Biomechanics Laboratory,
Swiss Federal Institute of Technology,
1015 Lausanne, Switzerland
E-mail: schuster@bioeng.ucsd.edu
Tel.: +1-858-8220785
Fax: +1-858-5343658

J.-L. Bény
Department of Zoology and Animal Biology,
Sciences III, 30 quai E. Ansermet,
1211 Geneva 4, Switzerland

Present address: AlexanderSchuster
Whitaker Institute of Biomedical Engineering,
Department of Bioengineering,
University of California, San Diego,
9500 Gilman Drive, La Jolla,
CA, 92093-0427, USA

Keywords Calcium ion dynamics · Endothelium-derived hyperpolarizing factor · Epoxyeicosatrienoic acids · Membrane potential · Potassium ion channels

Abbreviations BK_{Ca} channel: large-conductance calcium-sensitive potassium channel · Ca^{2+}: calcium ion, generally free intracellular concentration · EC: endothelial cell · EDHF: endothelium-derived hyperpolarizing factor · EETs: epoxyeicosatrienoic acids · IP_3: inositol 1,4,5-trisphosphate · *I-V* curve: current-potential relationship · NO: nitric oxide · P_o: open-state probability · PMCA: plasmalemmal Ca^{2+}-ATPase · SK_{Ca} channel: small-conductance calcium-sensitive and apamin-insensitive potassium channel · SERCA: sarcoplasmic/endoplasmic reticulum Ca^{2+}-ATPase · SMC: smooth muscle cell · SR: sarcoplasmic/endoplasmic reticulum · V_m: membrane potential

Introduction

Situated at the interface between blood and the muscular media of the vessel, endothelial cells play a major role in the local control of the vascular tone by producing vasoactive agents like nitric oxide (NO), prostacyclin, and the still unidentified endothelium-derived hyperpolarizing factor (EDHF). The activation of endothelial cells by circulating mediators leads to an intracellular calcium concentration ($[Ca^{2+}]_i$) rise, due to Ca^{2+} release from intracellular Ca^{2+} stores and Ca^{2+} influx from the extracellular space (Himmel et al. 1993). In many cases, this effect is associated with a membrane hyperpolarization (for review see Nilius et al. 1997), which plays an important role in the production of endothelial vasoactive substances by increasing the (electrochemical) driving force for Ca^{2+} entry (Luckhoff and Busse 1990).

The peptide bradykinin is an endothelium-dependent vasodilator for most arteries, including the pig coronary artery, producing NO and EDHF as relaxing agents (Pacicca et al. 1992). In coronary artery endothelial cells,

this peptide produces a transient hyperpolarization associated with an increase of $[Ca^{2+}]_i$ (Baron et al. 1996; Brunet and Beny 1989; Sharma and Davis 1994). The intracellular second messenger cascade triggered by bradykinin-receptor binding involves the activation of phospholipase C and the production of inositol 1,4,5-trisphosphate (IP_3), which in turn release Ca^{2+} from IP_3-sensitive Ca^{2+} stores (Farmer et al. 1992; Regoli et al. 1994). Using whole-cell patch-clamp experiments, intracellular microelectrode membrane potential recordings, and intracellular Ca^{2+} measurements using conventional fluorescence microscopy with Fura-2 in endothelial cells in primary culture, Sollini and coworkers (Baron et al. 1996, 1997; Frieden et al. 1999; Sollini et al. 2002) proposed a phenomenological model for the bradykinin response. This model takes into account intra- and extracellular Ca^{2+} sources, two K^+ channels (a large-conductance channel, BK_{Ca}, and a small-conductance, apamin-insensitive K^+ channel, SK_{Ca}, both being Ca^{2+}-sensitive), a non-selective cation channel permeable to Na^+, K^+, and Ca^{2+}, and the membrane potential (see Fig. 1).

While, in this way, many aspects of the endothelial-cell physiology and pharmacology have already been measured, some quantities, like the measurement of the individual K^+ channel contributions in the overall response with membrane potential free to vary, have not been possible to determine experimentally. Furthermore, the interpretation of the results has been based on hypothetical mechanisms. In order to test these hypotheses, a biophysical model based upon them can be constructed, thus allowing us to compare whether the simulated results are in accordance with the experimental ones. This would then confirm both the validity of the initial hypotheses and the validity of the model. Furthermore, predictions as to not yet measured quantities could be made, and the model be tested by carrying them out.

The purpose of this study is thus to develop a biophysical model of the membrane potential response of pig coronary artery endothelial cells in primary culture upon bradykinin stimulation. This will allow us to cross-check the above-mentioned phenomenological model, as well as to test the implication of epoxyeicosatrienoic acids (EETs) as proposed by Baron et al. (1997), and to predict the individual K^+ channel contributions in the overall current. Furthermore, the model will allow us to calculate the amount of K^+ released upon bradykinin stimulation. This is pertinent in the context of the proposed hypothesis (Edwards et al. 1998) that K^+ could be, or at least contribute to, the EDHF phenomenon.

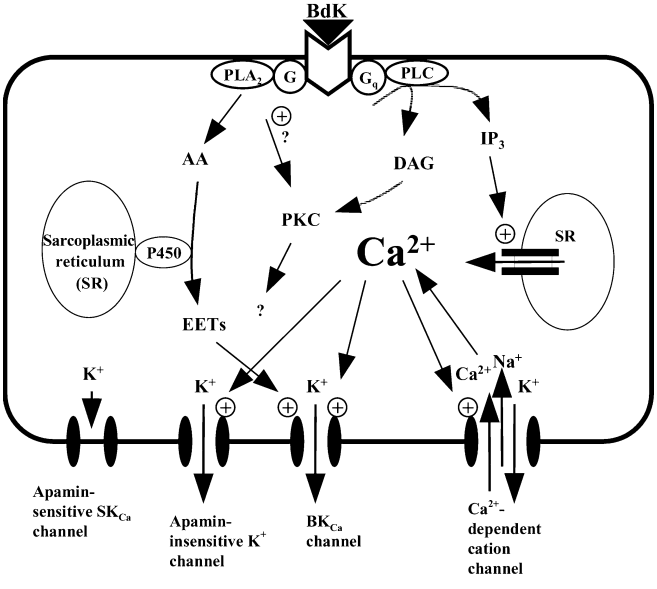

Fig. 1 Bradykinin stimulates different types of channels: the large-conductance BK_{Ca} channel, the apamin-insensitive small-conductance SK_{Ca} channel, and a non-selective cation channel responsible for the Ca^{2+} entry. Apamin-sensitive SK_{Ca} channels are not gated by bradykinin. *AA*: arachidonic acid; *BdK*: bradykinin; *DAG*: diacylglycerol; *EETs*: epoxyeicosatrienoic acids; *G*: G protein; *IP_3*: inositol 1,4,5-trisphosphate; *P450*: P450 cytochrome oxidase; *PKC*: phosphokinase C; *PLA_2*: phospholipase A_2; *PLC*: phospholipase C; *SR*: sarcoplasmic/endoplasmic reticulum

Experimental background to the model

This model is based upon the experiments described essentially in the following publications: Baron et al. (1996, 1997), Frieden et al. (1999), and Sollini et al. (2002). The following sections are a short summary of the experimental methods and the main results.

Experimental methods

The experimental methods have been described in detail previously (Baron et al. 1996, 1997; Frieden et al. 1999). In short, endothelial cells from domestic pig *Sus scrofa* coronary arteries were used after 2–5 days of primary culture. Single-channel or whole-cell recordings were done using the standard patch-clamp technique in the cell-attached, inside-out, or whole-cell configurations, using a patch-clamp amplifier. To determine the current-potential relationships, repetitive 300 ms voltage pulses were applied throughout the recording, usually reaching 30, 50, and 80 mV above the holding potential. Results were normalized using the membrane capacitance. Membrane potential was measured with a conventional glass microelectrode.

Intracellular calcium was measured using conventional fluorescence microscopy with Fura-2. The obtained fluorescence ratio was then calibrated using the method described by Grynkiewicz et al. (1985). The dissociation constant K_d of Fura-2 for Ca^{2+} was taken as 225 nM.

Main results

Bradykinin produced a transient hyperpolarization of 20 mV accompanied by a synchronous transient increase

of $[Ca^{2+}]_i$ from about 10 to 1000 nM. Using the cell-attached and inside-out modes of the patch-clamp technique, bradykinin (94 nM) was found to activate three types of Ca^{2+}-dependent channels: a large-conductance K^+ channel sensitive to iberiotoxin (BK_{Ca}, 285 pS in high symmetrical K^+), whose open-state probability was increased by depolarization, a small-conductance, apamin-insensitive but charybdotoxin-sensitive K^+ channel (SK_{Ca}, 10 pS), and an inwardly rectifying non-selective cation channel (44 pS in high symmetrical K^+). The 285 pS K^+ channel was half-maximally activated by cytosolic Ca^{2+} levels of 1.6 and 4.5 μM at +10 and −30 mV, respectively. Such local concentrations cannot be reached in the presence of bradykinin, which induces a mean maximal cytosolic Ca^{2+} rise of 1.3 μM at −50 mV. However, the study of the effect of EETs, which have been described as EDHFs (Campbell et al. 1996; Hecker et al. 1994), has shown that they potentiate the endothelial BK_{Ca} channel activation by Ca^{2+}. In the presence of EETs, the open-state probability of the BK_{Ca} is enhanced already at a lower intracellular Ca^{2+} concentration, suggesting that the BK_{Ca} channel will release K^+ already at lower Ca^{2+} concentrations, thus leading to an earlier hyperpolarization. The small-conductance, apamin-insensitive K^+ channel was half-maximally activated by cytosolic Ca^{2+} levels of 600–700 nM and was found to be membrane potential independent. The (non-selective) cation channel appeared to be about as sensitive to Ca^{2+} as the small-conductance K^+ channel, with a half-maximal open-state probability induced by 0.7 μM Ca^{2+} on the intracellular side of the membrane. It is permeable to divalent cations such as Ca^{2+} with nearly the same permeability (P) as monovalent cations (P_K:P_{Na}:P_{Ca} = 1:1:0.7) and is equally membrane potential independent. In the absence of extracellular Ca^{2+}, the bradykinin-induced increase in cytosolic free Ca^{2+} was shortened temporally by 52% and reduced in amplitude by 88%, whereas the bradykinin-induced hyperpolarization was not significantly reduced in amplitude but was shortened by 70%, thus illustrating the major role of Ca^{2+} influx in endothelial cell activation by kinins. We hypothesize that the cation channel contributes to increase the cytoplasmic Ca^{2+} level, thus activating Ca^{2+}-dependent K^+ channels, and triggering membrane hyperpolarization when the endothelial cells are stimulated by a vasoactive agonist such as bradykinin.

Using a whole-cell patch-clamp and knowing that the capacity of an endothelial cell is 25.8 ± 1.6 pF, the whole-cell conductivity was found to be 268.5 ± 18.7 pS/pF during bradykinin stimulation. This current was found to be almost exclusively a K^+ current, as the current reversal potential of −73.7 ± 1.0 mV is close to the K^+ equilibrium potential of −80 mV. In the absence of stimulation, the current-potential relationship showed the existence of a "residual" current, which had a conductivity of 35–40 pS/pF, with a reversal potential of approximately −30 mV. Since the reversal potential of this current is much higher than that of K^+, this implies the involvement of other ions, possibly an outward Cl^- current, an inward Na^+ current, an inward K^+ pumping, etc.

The model

This model is based upon two key parameters: intracellular Ca^{2+} concentration and membrane potential. The dynamics of the former will depend upon the Ca^{2+} release from the sarcoplasmic/endoplasmic reticulum (SR) triggered by IP_3 (which is formed upon bradykinin stimulation), as well as upon a Ca^{2+} entry from the extracellular medium through Ca^{2+}-dependent cation channels. Membrane potential is mainly determined by transmembrane K^+ currents, the rest of the transmembrane fluxes being grouped together in a "residual" current. All model parameters are summarized in Table 1.

The first part of the model, which concerns the Ca^{2+} dynamics, is rather speculative. Indeed, the Ca^{2+} mechanisms have not been tested in the present study. Its purpose is to provide a plausible equation for the Ca^{2+} dynamics which fits the experimental data, and which can then be used in the modelling of the K^+ current.

Ca^{2+} dynamics

The sarcoplasmic/endoplasmic reticulum

Little is known so far about the duration and amplitude of the IP_3 peak elicited upon bradykinin stimulation, or about the resulting Ca^{2+} release from the SR, but it is known that IP_3 disintegrates in cytosolic extracts with a half-life of about 4 s (Berridge 1987; Sims and Allbritton 1998; Wang et al. 1995), giving rise to a decay constant

Table 1 Set of parameters used in the model for the endothelial cell response to bradykinin. All parameters result from fits of the experimental data

Model parameters	
k_{IP3}	0.1733 s^{-1}
$m3_{IP3}$	4
$m4_{IP3}$	55
A	0.211
$k_{SR,rel}$	180 nM/s
$m3_{SR}$	1.1
$m4_{SR}$	0.3
k_{PMCA}	0.679 nM/s
$m3_{PMCA}$	−6.19
$m4_{PMCA}$	0.39
G_{cat}	0.66 nM/(mV s)
E_{Ca}	50 mV
$m3_{Cat}$	−6.18
$m4_{Cat}$	0.37
G_{tot}	6927 pS
G_R	955 pS
E_K	−80 mV
V_{rest}	−31.1 mV

of $k_{IP3} = (\ln 2)/4 = 0.1733\ s^{-1}$, and that norepinephrine gives rise to an IP_3 peak with a FWHM of about 20–30 s (Itoh et al. 1992). The IP_3 peak maximum has thus been normalized to one, and the corresponding SR release fitted so as to reproduce the experimental Ca^{2+} dynamics.

The equations governing the IP_3 stimulation of the SR can be written as:

$$\frac{d(IP_3[t])}{dt} = A\left[1 + \tanh\left(\frac{-t + m3_{IP3}}{m4_{IP3}}\right)\right] - k_{IP3}IP_3[t] \quad (1)$$

The first term in this equation gives rise to an approximately exponential decrease of IP_3 formation rate with time, as only the decreasing part of the hyperbolic tangent is being used ($m4_{IP3} > m3_{IP3}$). Other kinds of functions could also be used, like for example the (decreasing) exponential function, but in the absence of more precise experimental data, one cannot say which one is better. The hyperbolic tangent has been chosen here in order to be coherent with the rest of the equations where hyperbolic tangents are especially useful (see later). The second term in Eq. (1) is a classical disintegration. Taken together, these two contributions give rise to an IP_3 peak.

The resulting Ca^{2+} release from the SR has been supposed to be positively correlated to the IP_3 concentration (sigmoidal relationship). Furthermore, given the diffusion coefficients for Ca^{2+} and IP_3 (13–65 $\mu m^2/s$ and 283 $\mu m^2/s$, respectively, in cytosolic extracts of *Xenopus laevis* oocytes (Allbritton et al. 1992), and given the characteristic size of an endothelial cell (about 500 μm^2), and supposing that IP_3 is formed uniformly along the cell membrane, one can thus consider that the diffusion time for IP_3 is negligible. The Ca^{2+} release from the SR will thus be considered to be immediate upon stimulation by bradykinin. Given the respective Ca^{2+} concentrations of the SR and the cytosol, one can suppose in a first approximation that the SR Ca^{2+} concentration remains constant during bradykinin stimulation, thus giving rise to a constant driving force. This hypothesis is confirmed by noting that a subsequent substance P (another peptide leading to Ca^{2+} release from the SR) stimulation of the cell gives rise to an almost unchanged Ca^{2+} response as compared with an initial substance P stimulation.

In this case, which corresponds to the experimental situation of the stimulation of the cells in the absence of extracellular Ca^{2+} (Fig. 2), there are two fluxes: a Ca^{2+} release from the SR and a Ca^{2+} extrusion (Eq. 2). The Ca^{2+} release from the SR depends only on the IP_3 concentration: in the absence of IP_3, there is no Ca^{2+} release, and when all the IP_3 receptors are saturated, a maximum Ca^{2+} release is reached (this is a simplification; see also Discussion). A sigmoidal relationship described by a hyperbolic tangent thus describes best the relationship between IP_3 concentration and Ca^{2+} release from the SR (first term in Eq. 2). Similarly, concerning

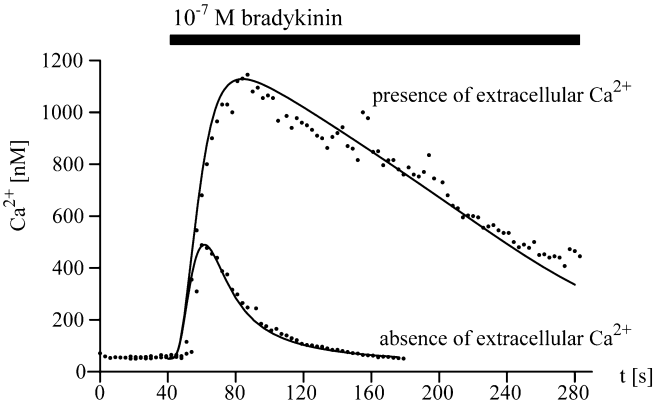

Fig. 2 Calcium dynamics stimulated by 100 nM bradykinin as a function of time, both in the presence and absence of extracellular calcium. Experimental data points from Frieden et al. (1999). The model predictions are the *solid curves*

the Ca^{2+} extrusion, in the absence of intracellular Ca^{2+}, no Ca^{2+} can be extruded, and when all the Ca^{2+} pumps are saturated, a maximum Ca^{2+} extrusion is achieved. The sigmoidal relationship again best represents this situation (second term in Eq. 2)[1]:

$$\frac{d(Ca[t])}{dt} = \frac{k_{SR,rel}}{2}\left[1 + \tanh\left(\frac{IP_3[t] - m3_{SR}}{m4_{SR}}\right)\right] - \frac{k_{PMCA}}{2}\left[1 + \tanh\left(\frac{\log(Ca[t]) - m3_{PMCA}}{m4_{PMCA}}\right)\right] \quad (2)$$

where $m3_{SR}$ (= 1.1) gives the half-activation of the Ca^{2+} release from the SR. k_{PMCA} (= 0.679 nM/s), $m3_{PMCA}$ (= −6.19), and $m4_{PMCA}$ (= 0.39) have been determined from the fit of the Ca^{2+} dynamics (decrease) in the presence and absence of extracellular Ca^{2+}.

The cation channel—Ca^{2+} dynamics in the presence of extracellular Ca^{2+}

The open-state probability of the non-selective cation channel depends upon the intracellular [Ca^{2+}] only. In particular, it is independent of the membrane potential (Sollini et al. 2002), implying that the Ca^{2+} dynamics and the membrane potential are almost uncoupled, except for the electrochemical driving gradient of the calcium influx through the cation channel, a hyperpolarization increasing the Ca^{2+} gradient, and thus the Ca^{2+} influx.

The equation for the Ca^{2+} dynamics is the same as above (Eq. 2), only that an additional term for the cation channel is added:

[1] The logarithm of the Ca^{2+} concentration is being used here as the cation channel has also a sigmoidal relationship for its open-state probability as a function of the $\log(Ca^{2+})$. Using a different form of the equation for the Ca^{2+} extrusion and the Ca^{2+} entry via the cation channel would lead to an impossibility to fit the experimental data satisfactorily.

$$J_{cat} = G_{cat}(E_{Ca} - V_m[t]) \times \frac{1}{2}\left[1 + \tanh\left(\frac{\log(Ca[t]) - m3_{cat}}{m4_{cat}}\right)\right] \quad (3)$$

The hyperbolic tangent is the result of a fit on experimental data, yielding in this way the EC_{50} activation value of 785.58 nM. $G_{cat} = 0.66$ nM/(mV s) corresponds to the (whole-cell) cation channel conductivity, and E_{Ca} is the Ca^{2+} equilibrium potential (= 116 mV).

The calcium dynamics depend thus upon three different fluxes: J_{SR}, the Ca^{2+} release from the SR (first term in Eq. 2), J_{cat}, the Ca^{2+} entry through the cation channel (Eq. 3), and J_{PMCA}, the extrusion of Ca^{2+} (either via the PMCA or via the SR, second term in Eq. 2). In order to produce a Ca^{2+} peak, the calcium release ($J_{SR,max}$ in the absence of extracellular Ca^{2+} or $J_{SR,max} + J_{cat}$ in the presence of extracellular Ca^{2+}) must be greater than the extrusion rate (J_{PMCA}), while at the same time the calcium influx through the cation channel (J_{cat}) needs to be smaller than J_{PMCA} (otherwise, since the cation channel open-state probability depends only upon the $[Ca^{2+}]_i$, and not upon membrane potential, the Ca^{2+} could never decrease again). It is the overlap of these fluxes which determines the length and amplitude of the resulting Ca^{2+} peak.

Currents and membrane potential

The current activated during bradykinin stimulation has a reversal potential very close to the K^+ equilibrium potential, and only the K^+ current dominates, other currents being negligible; at rest, the reversal potential has shifted to a less hyperpolarized state, thus indicating the implication of other ions in this "residual" current.

The K^+ current $IK[t]$ consists of two distinct contributions: the BK_{Ca} channel, a large-conductance channel activated by Ca^{2+} and membrane potential, and the apamin-insensitive SK_{Ca} channel, a small-conductance channel, only activated by Ca^{2+}:

$$IK[t] = G_{tot}(V_m[t] - E_K)(0.4P_oBK_{Ca}[Ca[t], V_m[t]] + 0.6P_oSK_{Ca}[Ca[t]]) \quad (4)$$

where G_{tot} is the total potassium channel conductivity, E_K is the K^+ equilibrium potential, P_oBK_{Ca} is the open-state probability of the BK_{Ca} channel, and P_oSK_{Ca} is the open-state probability of the SK_{Ca} channel. In the supramaximal presence of Ca^{2+} (1200 nM) this current consists of 40% of a current through the BK_{Ca} channel and of 60% of a current through the apamin-insensitive SK_{Ca} channel, hence the factors 0.4 and 0.6 in this equation (see Frieden et al. 1999). This fact is derived from the experimental *I-V* (current-voltage) curves, where a selective blockade of the BK_{Ca} channel with iberiotoxin decreases the channel conductivity by 40%. In addition, iberiotoxin plus charybdotoxin (which blocks the SK_{Ca} channels) abolished the current induced by bradykinin.

The open-state probability of the BK_{Ca} channel depends both upon the intracellular Ca^{2+} concentration and the membrane potential. Taking together the experimental data which give the P_oBK_{Ca} either as a function of Ca^{2+} for different membrane potentials, or as a function of V_m for different Ca^{2+} concentrations (in the absence of EETs), allows us to construct a two-dimensional fit of the P_oBK_{Ca}. The potentiating effect of EETs is taken into account by shifting the P_oBK_{Ca} either with respect to Ca^{2+} (by about a factor 30, for an unchanged V_m dependence), or V_m (by 43 mV, for an unchanged Ca^{2+} dependence), or a combination of both, by fitting the resulting theoretical *I-V* curves on the experimental data.

The "corrected" differential equation governing the V_m dynamics, replacing Eq. (4), then becomes:

$$IK[t] = G_{tot}(V_m[t] - E_K)(0.4P_oBK_{Ca}[Ca[t] \times 30,\ V_m[t]] + 0.6P_oSK_{Ca}[Ca[t]]) \quad (5)$$

The cation channel contribution to the K^+ current is being neglected here, as there is also a Na^+ current through the cation channel, of a similar amplitude, and in the opposite direction. The net effect of these two currents is negligible. Similarly, the contribution of the Ca^{2+} influx has not been included in the total current ($IK[t] + IR[t]$), as it is negligible compared to the potassium current.

The repolarizing current after cell hyperpolarization, the so-called "residual" current, consists either of an inward positive current or an outward negative current, possibly an outward Cl^- current, an inward Na^+ current, or an inward K^+ pumping, etc. These contributions have been grouped together into the following equation:

$$IR[t] = G_R(V_m[t] - V_{rest}) \quad (6)$$

where G_R is the residual current conductivity and V_{rest} is the membrane resting potential.

The resulting membrane potential dynamics are then given by:

$$\frac{dV_m}{dt} = -\frac{1}{C}(IK[t] + IR[t]) \quad (7)$$

where C is the membrane capacitance.

Results

Ca^{2+} dynamics in the presence or absence of extracellular calcium

Using Eq. (1) for the IP_3 dynamics, Eq. (2) for the case in the absence of extracellular calcium, and combining Eqs. (2) and (3) for the case in the presence of extracellular calcium, the Ca^{2+} dynamics were fitted as a function of time, as shown in Fig. 2. In the absence of extracellular Ca^{2+}, only the SR releases Ca^{2+}, and this is then rather quickly pumped out of the cytoplasm

[either via the SR Ca^{2+}-ATPase (SERCA) or the PMCA]. On the other hand, when Ca^{2+} can enter the cell from the extracellular space, a much larger Ca^{2+} increase is produced, and a slower decrease, since in this case the net Ca^{2+} outflux is the pumping rate of the SERCA and the PMCA minus the still non-zero Ca^{2+} influx through the cation channel. The curve predicted by the model fits the experimental data available almost perfectly.

Open-state probability of the potassium channels

Both the large conductance BK_{Ca} channel and the small conductance (apamin-insensitive) SK_{Ca} channel depend upon the intracellular Ca^{2+} concentration, but only the BK_{Ca} channel depends also upon membrane potential. The experimental data available give the open-state probability P_o of the BK_{Ca} channel as a function of intracellular Ca^{2+} for two different holding potentials (Fig. 3A, showing an increase in open-state probability with increasing Ca^{2+}), and as a function of membrane potential for three different intracellular Ca^{2+} concentrations (2 mM, 3 μM, and 1 μM; Fig. 3B, showing an increase in open-state probability with increasing membrane potential).

Fig. 3A–D Ca^{2+} and membrane potential dependence of the BK_{Ca} channel. **A** Fits of the open-state probability (P_oBK_{Ca}) expressed as a function of intracellular Ca^{2+} concentration at two holding potentials, −30 mV (*triangles*) and +10 mV (*dots*). The experimental data were recorded from inside-out patches in the presence of various Ca^{2+}-containing EGTA-buffered solutions (Baron et al. 1996). **B** Fits of the open-state probability expressed as a function of holding potential in the presence of various intracellular Ca^{2+} concentrations: 2 mM (*dots*), 3 μM (*triangles*), and 1 μM (*squares*). **C** Fit of the relationship between the pCa_{50} value ($\log[Ca^{2+}]$ EC_{50} value) for the half-activation of the BK_{Ca} channel as a function of membrane potential. **D** Two-dimensional fit of the BK_{Ca} open-state probability as a function of both Ca^{2+} and V_m

The experimental data in Fig. 3A and B have been fitted using a hyperbolic tangent fit, x being the variable to be fitted (e.g. Ca^{2+} concentration or membrane potential):

$$P_o = \frac{1}{2}\left(1 + \tanh\left[\frac{x - m_3}{m_4}\right]\right) \tag{8}$$

where m_3 and m_4 are parameters determined by the fit (m_3 corresponds to the half-activation and m_4 to the "spread" of the curve).

Extracting from these graphs the Ca^{2+} EC_{50} value (open-state probability 50%) as a function of membrane potential yields an exponential relationship between the Ca^{2+} EC_{50} value and V_m (Fig. 3C). Taken together, this allowed us to construct a two-dimensional fit of the BK_{Ca} open-state probability as a function of both intracellular Ca^{2+} and V_m (Fig. 3D). The equation of this fit (Eq. 9) for the P_oBK_{Ca} was then used in Eq. (5) in order to calculate the K^+ current:

$$P_oBK_{Ca} = \frac{1}{2}\left(1 + \tanh\left[\frac{\left(\log[Ca^{2+}] - c\right)(V_m - b) - a}{m_3\left(V_m + a\left(\log[Ca^{2+}] - c\right) - b\right)^2 + m_4}\right]\right) \tag{9}$$

where $a = 53.3$, $b = -80.8$, $c = -6.4$, $m_3 = 1.32\times10^{-3}$, and $m_4 = 0.30$.

The fitted values yield a half-activation Ca^{2+} concentration of 3944 nM at −30 mV, and of 1543 nM at +10 mV. Notice, however, that these values have been obtained in the absence of EETs, which strongly decrease these half-activation values (approximately by a factor 30, see Discussion). The half-activation membrane potentials resulting from these fits are −66.6, −23.6, and +31.4 mV for a Ca^{2+} concentration of 2 mM, 3 μM, and 1 μM, respectively.

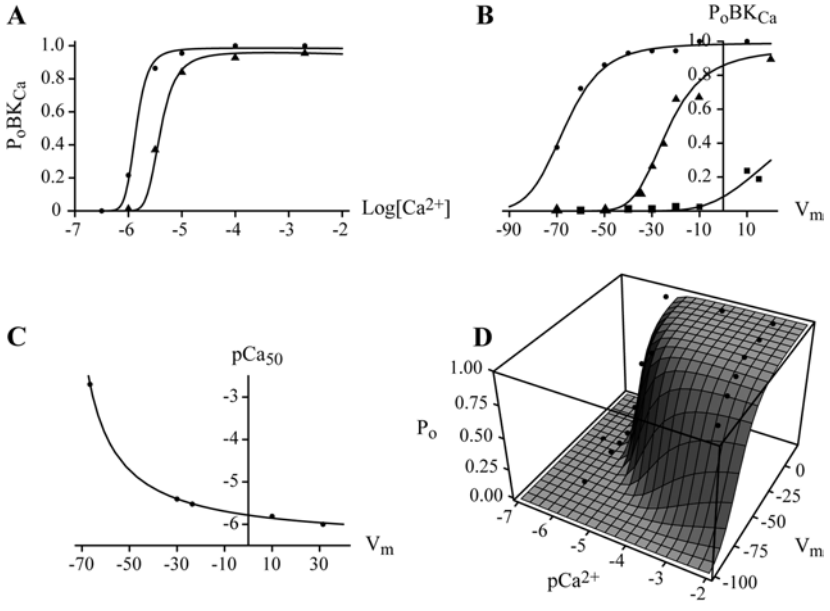

The apamin-insensitive SK_{Ca} channel open-state probability depends only upon the intracellular Ca^{2+} concentration, the fit of the experimental data (Sollini et al. 2002) yielding a half-activation concentration for Ca^{2+} of 529 nM (fitted value). There is no dependence of the open-state probability of this channel upon membrane potential.

Effect of currents on membrane potential

Results obtained for the membrane potential dynamics in the absence of extracellular Ca^{2+} are in excellent agreement with experimental values, showing that the hypotheses made so far seem to be correct (Fig. 4A). Indeed, even though the absolute values do not correspond exactly with the values obtained by Baron et al. (1996, Fig. 9), where the resting potential was quite far from the average value they reported (about −15 mV, to be compared with the -31.1 ± 1.6 mV they report for the average membrane resting potential), the amplitude of the hyperpolarization is very similar: −35 mV (average) in the experimental case and −32.5 mV in the model. Furthermore, the dynamics are also in good agreement, as the duration of the hyperpolarization, as estimated from the FWHM of the peak, is almost the same in the two cases.

Trying to include a term corresponding to the K^+ current through the cation channel produced an immediate very clear hyperpolarization at the K^+ equilibrium potential. It is thus essential, as supposed previously, that this K^+ current through the cation channel is almost perfectly counterbalanced by a Na^+ current.

Using the same equations, the hyperpolarization resulting from the Ca^{2+} increase in the presence of extracellular Ca^{2+} upon bradykinin stimulation has been determined (Fig. 4B). The hyperpolarization amplitude obtained (−38.4 mV) is again very close to the experimental average of −35 mV.

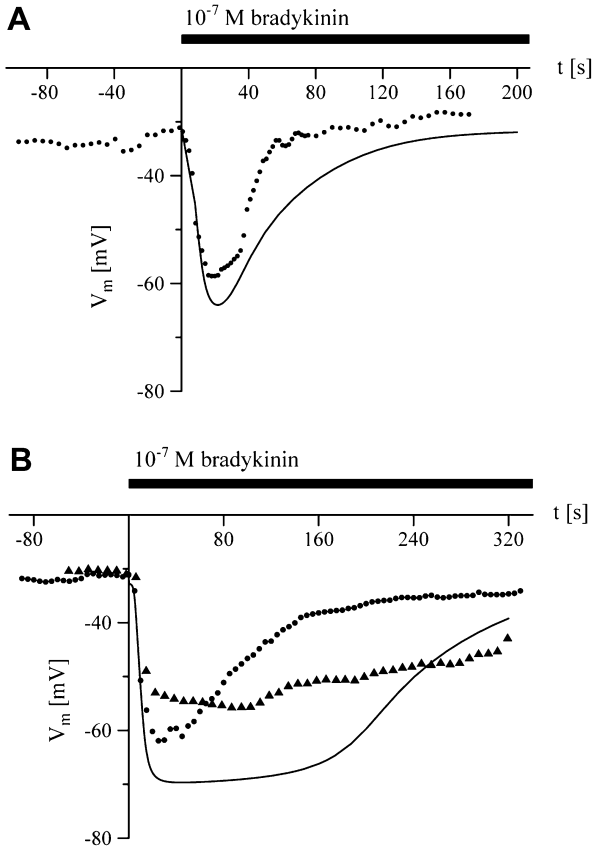

Fig. 4 Membrane hyperpolarization upon bradykinin stimulation in (**A**) the absence and (**B**) the presence of extracellular Ca^{2+}. Experimental data (from Baron et al. 1996) have been shifted so as to begin with the same membrane resting potential as in the model (*solid line*), corresponding to the average reported. The model prediction is the *solid curve*. In **B**, experimental data points from two different experiments have been shown (*dots* and *triangles*, respectively)

Predictions for the actual BK_{Ca} and SK_{Ca} currents

Figure 5 shows the contributions of the three different currents (BK_{Ca}, SK_{Ca}, and residual current) as predicted by the model in the presence and absence of extracellular Ca^{2+}, as well as the resulting total current. The BK_{Ca} channel does not appear to contribute very much to the overall current. Indeed, upon stimulation, even though the increase in intracellular Ca^{2+} has a tendency to increase the P_oBK_{Ca}, this effect is less pronounced than the resulting hyperpolarization, which closes the channel very quickly. The resulting effect is an almost negligible contribution of this channel to the overall bradykinin response, even in the presence of EETs. This also implies that EETs are not important in the bradykinin electrophysiological response.

The model predicts very similar current-voltage relationships (for the maximal presence of Ca^{2+} of 1200 nM) as obtained experimentally (Frieden et al. 1999), yielding exactly the same conductance for the BK_{Ca} channel (Fig. 6) as Frieden et al. (1999, Fig. 3C). The black and gray solid curves in Fig. 6A correspond to the control current and the current in the presence of iberiotoxin, respectively, in the experimental curves of Frieden et al. (1999, Fig. 3C). These *I-V* curves are the same as those obtained experimentally only if the EETs are taken into account (*I-V* curves in the absence of EETs not shown), which underlines the importance of these factors.

Total K^+ released during bradykinin stimulation

When integrating the total K^+ current during bradykinin stimulation, this yielded a total charge $Q = \int IK[t]dt = 1.94\times10^{-9}$ C in the case of the absence of extracellular Ca^{2+}, and 7.48×10^{-9} C in the case of the presence of extracellular Ca^{2+}. This corresponds to a total K^+ quantity released of 2.0×10^{-14} and 7.7×10^{-14} moles, respectively.

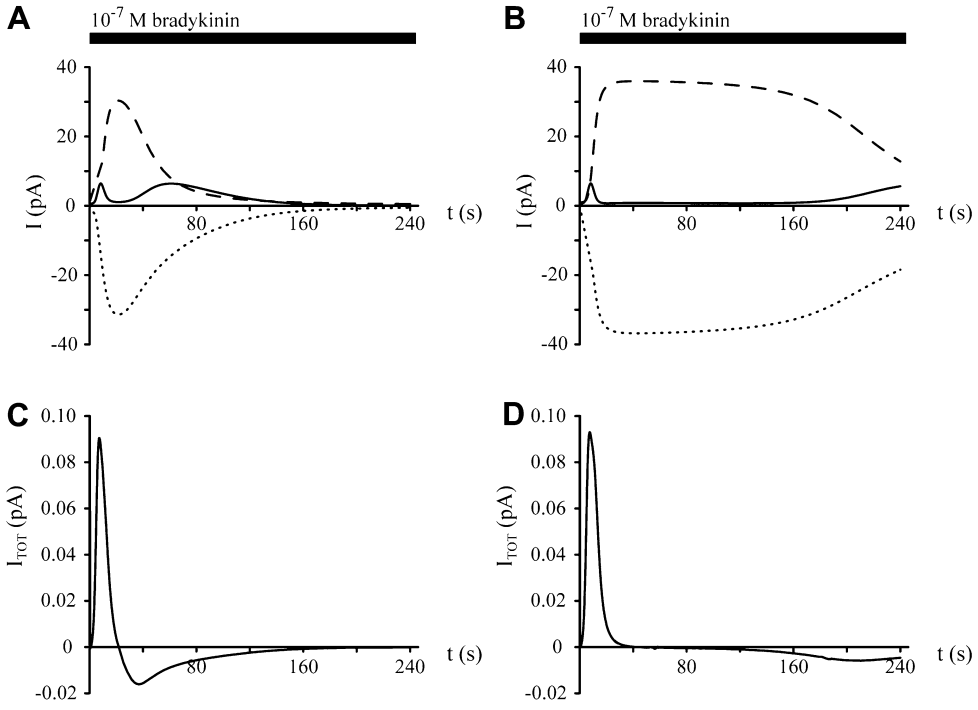

Fig. 5 Individual membrane current contributions upon bradykinin stimulation in the absence (**A**) and presence (**B**) of extracellular Ca^{2+}, as predicted by the model (in the presence of EETs). *Solid line*: K^+ current passing through the BK_{Ca} channel; *dashed line*: K^+ current passing through the SK_{Ca} channel; *dotted line*: residual current. **C**, **D** Total transmembrane current as a function of time

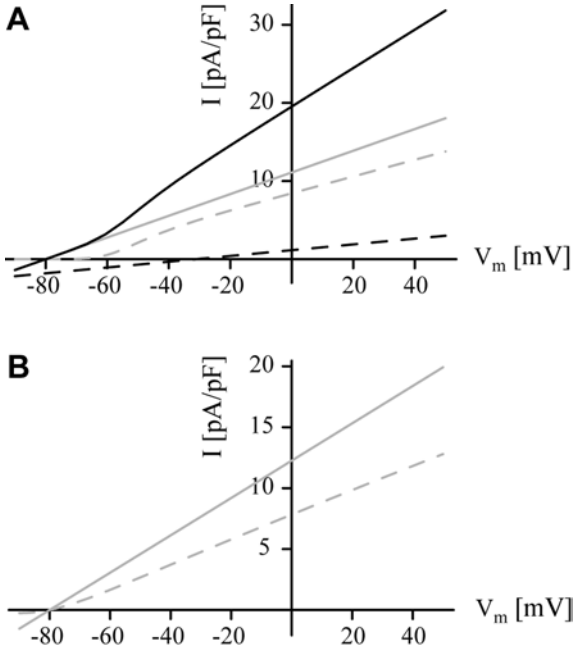

Fig. 6A, B Current-potential curves in the presence of 1200 nM Ca^{2+} during bradykinin stimulation, as predicted by the model (in the presence of EETs). The total current (*black solid line*) is composed of the BK_{Ca} current (*gray dashed line*) and the apamin-insensitive SK_{Ca} current (*gray solid line*). The "residual" current is shown by the *black dashed curve*. **A** The BK_{Ca} open-state probability has been shifted with respect to Ca^{2+} by a factor 30. **B** Almost the same result is obtained when shifting the BK_{Ca} open-state probability as a function of V_m, and not Ca^{2+}, in order to take into account the EETs

Knowing that the surface of an endothelial cell in primary culture is about $880 \pm 100\ \mu m^2$ ($n = 5$, determined from electron micrographs), and that its height is approximately 4 μm (measured on non-confluent, cultured cells), and considering the cell as a cone, this gives a cell volume of 1173 μm^3. The K^+ quantity released corresponds thus to an intracellular K^+ concentration change of 17.0 mM and 65.6 mM, respectively. Concerning the intercellular space, whose thickness can be estimated in a first approximation at between 1 and 6 μm, this yields concentration changes in the extracellular space of 22.7 mM (1 μm thickness) to 3.8 mM (6 μm thickness) in the absence of extracellular calcium, and 87.5 mM (1 μm thickness) to 14.6 mM (6 μm thickness) in the presence of extracellular calcium. The resting extracellular K^+ concentration being about 5 mM, this K^+ release constitutes a significant K^+ concentration change.

On the other hand, considering the "intercellular space" between the ECs and the SMCs composed of the internal elastic lamina as a freely available space for K^+ diffusion is rather simplistic. Indeed, this lamina is generally thought to be an impermeable layer, even to water, except where there are fenestral pores (Tada and Tarbell 2000). The available space for the K^+ is therefore still smaller, leading to a still higher K^+ concentration around the ECs, and a decreasing concentration gradient towards the adventitia. However, the aim here is not to model the interstitial diffusion of K^+, and the simplistic approach given above allows us to obtain an order of magnitude.

Discussion

The aim of this model was to construct a rather simple set of equations which allows us to reproduce the observed experiments on cultured porcine coronary

artery endothelial cells within experimental accuracy, and to predict some new, not yet measured, quantities.

Calcium dynamics

The aim in the present paper was not to propose a complete set of equations for all steps of the complex calcium signalling, but rather to come up with a plausible equation which reproduces the experimental Ca^{2+} dynamics, and which could then be used in the calculation of the currents and membrane potential. Several simplifications have been carried out, like neglecting the Ca^{2+}-induced Ca^{2+} release phenomenon, neglecting the SR Ca^{2+}-release dependence of the IP_3 receptor upon Ca^{2+} (positive and negative biphasic dependence), considering the release immediate and neglecting any time necessary for diffusion, and especially not taking into consideration the compartmentalization of the cell. These refinements are nevertheless important only at a smaller time-scale, as the model achieves to reproduce the observed experimental dynamics rather well.

Indeed, the modelled Ca^{2+} responses in both the presence and the absence of extracellular Ca^{2+} agree very well with the experimental curves (Fig. 2). Many experimental parameters are known in this case, thus allowing a good reproduction of the experimental results, taking into account only the Ca^{2+} released from the SR and the Ca^{2+} entry through the cation channel. Certain hypotheses concerning the IP_3 dynamics had nevertheless to be made. The IP_3 dynamics consist of a production upon bradykinin stimulation, which decreases slightly with time, and a catabolism of IP_3, corresponding to the half-life of IP_3 as measured in cytosolic extracts. Both the decrease in production rate and the half-life of IP_3 are unknown parameters in the present study, and had to be adjusted so as to fit the Ca^{2+} dynamics in both the presence and the absence of extracellular Ca^{2+} (see also the subsection The sarcoplasmic/endoplasmic reticulum in the section The model, above).

Membrane potential dynamics

In this case, many biological constraints (measurements) exist on the model, leaving almost no unverified hypotheses, making the model very predictive with respect to currents. When looking more closely at the membrane potential dynamics (Fig. 4A, B), it appears that, in the absence of extracellular Ca^{2+}, the dynamics predicted by the model correspond rather well to the experimental observations. Indeed, even though the modelled hyperpolarization has a slightly greater amplitude than the experimental one, this can be explained due to the smaller Ca^{2+} peak in this particular experimental situation. Experimentally, there is a great variability in the response of the cells. This is due to the fact that cells in primary culture were used for the experiments, leading to an inherent biological variability. As the Ca^{2+} dynamics were not measured simultaneously with the V_m dynamics, nor even on the same cells, it is very natural that the model does not reproduce exactly the experimental Ca^{2+} and V_m dynamics, which for the model are obviously calculated simultaneously. Furthermore, difficulties in calibrating the Ca^{2+} measurement system give rise to greatly varying Ca^{2+} amplitudes among the different publications used (Baron et al. 1996, 1997; Frieden et al. 1999). The overall shape of the response is nevertheless always retained. As an example, one of the characteristics of the bradykinin-induced hyperpolarization is its increased duration in cultured cells as compared with cells in situ. The inherent variability of cultured cells is thus reflected also in the hyperpolarization durations observed. In this particular case, the modelled peak has a greater amplitude, which then naturally takes slightly longer in order to recover to the resting membrane potential. The shape of the V_m decrease is still very similar to the experimental one, thus showing that the proposed mechanisms are compatible with reality. Furthermore, it could be that EETs disintegrate rather quickly, too, so that the second peak in the BK_{Ca} current (as shown in Fig. 5A) is greatly attenuated. This would then increase the rate of hyperpolarization decrease.

Concerning the membrane potential dynamics in the presence of extracellular Ca^{2+}, Fig. 4B shows two experimental curves obtained, one with a rather quick decrease of V_m and one with a very slow V_m decrease. The curve predicted by the model is somewhat intermediate between these two extremes, with a plateau phase in the hyperpolarized state and then presenting a V_m decrease with a similar rate as that observed in the first experimental curve (dots). There is again a greater hyperpolarization predicted by the model than that observed experimentally. With a great variability being observed in the amplitude of the hyperpolarizations, as well as the corresponding Ca^{2+} dynamics, one can affirm here again that this greater hyperpolarization is due to the slightly greater Ca^{2+} peak forecast by the model, as compared with the experimental situation when these hyperpolarization curves were measured (Fig. 9, Baron et al. 1996; Baron et al. 1997; Frieden et al. 1999). Simultaneous measurements of Ca^{2+} and V_m dynamics would be required in order to be able to really conclude whether the model is fully valid in this case, or would require us to take into account some additional current.

K^+ currents

One of the questions addressed is: is the presence of EETs required in order to explain the experimental observations? Analysis of the BK_{Ca} open-state probability shows that they are indeed essential. The BK_{Ca} open-state probability in the absence of EETs, very well determined experimentally as a function of both

intracellular Ca^{2+} and V_m, has allowed us to construct a rather precise two-dimensional fit as a function of these two variables (Fig. 3). When using this open-state probability for the V_m dynamics, the model showed that, within the physiological range of Ca^{2+} and V_m, the BK_{Ca} channel would always be closed. Also, the predicted *I-V* curves (Fig. 6) do not fit the experimental data if some potentiating effect of the P_oBK_{Ca} is not considered. The candidate retained for this are the EETs, which are produced from arachidonic acid by cytochrome P450 mono-oxygenase on the SR, arachidonic acid production being also stimulated by bradykinin (Baron et al. 1997). Since these studies have been carried out using exogenous EETs, this only suggests, but does not prove, a physiological role of EETs. On the other hand, since BK_{Ca} channels contribute only very little to the overall bradykinin response, it follows that EETs do not play an important role in the resulting hyperpolarization.

The experimental data available do not allow us to conclude how to shift the two-dimensional open-state probability curve as a function of Ca^{2+} and V_m (only two experimental points are available for the BK_{Ca} open-state probability in the presence of EETs). It is thus not possible to know whether EETs create a greater Ca^{2+} sensitivity or a greater V_m sensitivity (increasing the open-state probability already for a more hyperpolarized state), which means, for the model, whether the curve is shifted on the Ca^{2+} axis or on the V_m axis, or a combination of both. Different combinations have been tried out with the model, showing that it does not really matter how the open-state probability curve is being shifted, as long as it is shifted by a factor of 30 for the Ca^{2+} sensitivity, or by 43 mV for the membrane potential dependence.

Could K^+ be EDHF?

In the rat hepatic and mesenteric artery, EDHF could be potassium ions released through the endothelial potassium channels (Edwards et al. 1998). In this case, the accumulation of K^+ in the myoendothelial space would stimulate the electrogenic Na^+/K^+-ATPase and/or the opening of the (Ba^{2+} sensitive) inwardly-rectifying potassium channels in the smooth muscle cells, thus leading to cell *hyperpolarization* (and not depolarization, as K^+ often does in many other types of cells). A necessary condition for the pertinence of this hypothesis is that the amount of K^+ released by the ECs is compatible with the concentration necessary to hyperpolarize and relax the vascular SMCs. Being based on actual current measurements, this model has allowed us to calculate reliably the amount of K^+ released by a cultured endothelial cell during bradykinin stimulation. It has shown that even though EETs are important in order to explain the experimental *I-V* curves obtained, they do not contribute significantly to the overall bradykinin response. On the other hand, the amount of K^+ ions released by the ECs during bradykinin stimulation is of the millimolar order of magnitude. In the hepatic artery from rat, the extracellular K^+ concentration ranges from 5 to 20 mM (Edwards et al. 1998). This means that the EC release enough K^+ to change the extracellular K^+ concentration significantly. This could then increase the activity of the SMC Na^+/K^+-ATPase, activating inwardly-rectifying K^+ channels on the SMCs, and relaxing the SMCs. The amount of K^+ released by the ECs being a necessary, though not sufficient, condition for the "K^+ = EDHF hypothesis", this does not prove that K^+ is EDHF, but it shows that the K^+ released by ECs during hyperpolarization due to bradykinin stimulation is compatible with a SMC relaxation.

Conclusion

The model constructed reproduces the experimental observations for both the Ca^{2+} and the V_m dynamics accurately, be it in the presence or absence of extracellular Ca^{2+}, thus implying that the hypotheses made are reasonable. It predicts that the current is mainly carried by the apamin-insensitive SK_{Ca} channel and the "residual" current, and that the BK_{Ca} channel participates very little in the bradykinin stimulation. Furthermore, it shows that EETs are required in order to explain the *I-V* curves obtained experimentally, but that they are not an essential component of the (electrophysiological) bradykinin response. Furthermore, sufficient K^+ is being released into the intercellular space during bradykinin stimulation so as to suggest that K^+ ions could contribute to the EDHF phenomenon in cultured porcine coronary artery endothelial cells.

Acknowledgements This work was supported by the Swiss National Science Foundation, grant FN 3152-61716.00.

References

Allbritton NL, Meyer T, Stryer L (1992) Range of messenger action of calcium ion and inositol 1,4,5- trisphosphate. Science 258:1812–1815

Baron A, Frieden M, Chabaud F, Beny JL (1996) Ca(2+)-dependent non-selective cation and potassium channels activated by bradykinin in pig coronary artery endothelial cells. J Physiol (Lond) 493:691–706

Baron A, Frieden M, Beny JL (1997) Epoxyeicosatrienoic acids activate a high-conductance, Ca(2+)-dependent K^+ channel on pig coronary artery endothelial cells. J Physiol (Lond) 504:537–543

Berridge MJ (1987) Inositol trisphosphate and diacylglycerol: two interacting second messengers. Annu Rev Biochem 56:159–193

Brunet PC, Beny JL (1989) Substance P and bradykinin hyperpolarize pig coronary artery endothelial cells in primary culture. Blood Vessels 26:228–234

Campbell WB, Gebremedhin D, Pratt PF, Harder DR (1996) Identification of epoxyeicosatrienoic acids as endothelium-derived hyperpolarizing factors. Circ Res 78:415–423

Edwards G, Dora KA, Gardener MJ, Garland CJ, Weston AH (1998) K^+ is an endothelium-derived hyperpolarizing factor in rat arteries. Nature 396:269–272

Farmer SG, Wilkins DE, Meeker SA, Seeds EA, Page CP (1992) Effects of bradykinin receptor antagonists on antigen-induced respiratory distress, airway hyperresponsiveness and eosinophilia in guinea-pigs. Br J Pharmacol 107:653–659

Frieden M, Sollini M, Beny J (1999) Substance P and bradykinin activate different types of KCa currents to hyperpolarize cultured porcine coronary artery endothelial cells. J Physiol (Lond) 519:361–371

Grynkiewicz G, Poenie M, Tsien RY (1985) A new generation of Ca^{2+} indicators with greatly improved fluorescence properties. J Biol Chem 260:3440–3450

Hecker M, Bara AT, Bauersachs J, Busse R (1994) Characterization of endothelium-derived hyperpolarizing factor as a cytochrome P450-derived arachidonic acid metabolite in mammals. J Physiol (Lond) 481:407–414

Himmel HM, Whorton AR, Strauss HC (1993) Intracellular calcium, currents, and stimulus-response coupling in endothelial cells. Hypertension 21:112–127

Itoh T, Seki N, Suzuki S, Ito S, Kajikuri J, Kuriyama H (1992) Membrane hyperpolarization inhibits agonist-induced synthesis of inositol 1,4,5-trisphosphate in rabbit mesenteric artery. J Physiol (Lond) 451:307–328

Luckhoff A, Busse R (1990) Calcium influx into endothelial cells and formation of endothelium-derived relaxing factor is controlled by the membrane potential. Pflugers Arch 416:305–311

Nilius B, Viana F, Droogmans G (1997) Ion channels in vascular endothelium. Annu Rev Physiol 59:145–170

Pacicca C, von der Weid PY, Beny JL (1992) Effect of nitro-L-arginine on endothelium-dependent hyperpolarizations and relaxations of pig coronary arteries. J Physiol (Lond) 457:247–256

Regoli D, Boudon A, Fauchere JL (1994) Receptors and antagonists for substance P and related peptides. Pharmacol Rev 46:551–599

Sharma NR, Davis MJ (1994) Mechanism of substance P-induced hyperpolarization of porcine coronary artery endothelial cells. Am J Physiol 266:H156–H164

Sims CE, Allbritton NL (1998) Metabolism of inositol 1,4,5-trisphosphate and inositol 1,3,4,5- tetrakisphosphate by the oocytes of *Xenopus laevis*. J Biol Chem 273:4052–4058

Sollini M, Frieden M, Beny JL (2002) Charybdotoxin-sensitive small conductance K(Ca) channel activated by bradykinin and substance P in endothelial cells. Br J Pharmacol 136:1201–1209

Tada S, Tarbell JM (2000) Interstitial flow through the internal elastic lamina affects shear stress on arterial smooth muscle cells. Am J Physiol Heart Circ Physiol 278:H1589–H1597

Wang SS, Alousi AA, Thompson SH (1995) The lifetime of inositol 1,4,5-trisphosphate in single cells. J Gen Physiol 105:149–171